Magnetohydrodynamics, Vol. 31, No. 3, 1995

MAGNETIC FIELD AND SEGREGATION DURING BRIDGMAN GROWTH

T. Alboussière,[2] A. C. Neubrand,[1]
J. P. Garandet,[1] and R. Moreau[2]

Axial segregation during horizontal Bridgman growth is investigated in the presence of a uniform axial magnetic field. Experiments have been carried out at several Hartmann numbers, as well as numerical and theoretical studies. These last methods predict that the Hartmann number has no influence on the axial segregation until it reaches a given value depending on the intensity of the buoyancy driving force. Then, segregation is slowly decreasing by increasing the Hartmann number. Although experimental results seem to show this reduction of axial segregation with magnetic field, they were not precise enough until now to confirm numerical and theoretical results.

1. Introduction

In the Bridgman method of controlled solidification, a liquid sample is withdrawn through a temperature gradient, hopefully as a single crystal. Buoyancy driven convection is often unavoidable, since density gradients are always present in the melt. Periodic or random motions are responsible for structural defects such as striations [1], but even a steady hydrodynamical regime may produce both lateral and radial segregations (homogeneity defects) [2]. Two methods exist in order to reduce these liquid motions: the microgravity environment (available for instance in the NASA space shuttle) that reduces the driving force, or the use of a steady magnetic field that stabilizes disturbances through the Joule effect and damps the fluid flow with the Lorentz force [3].

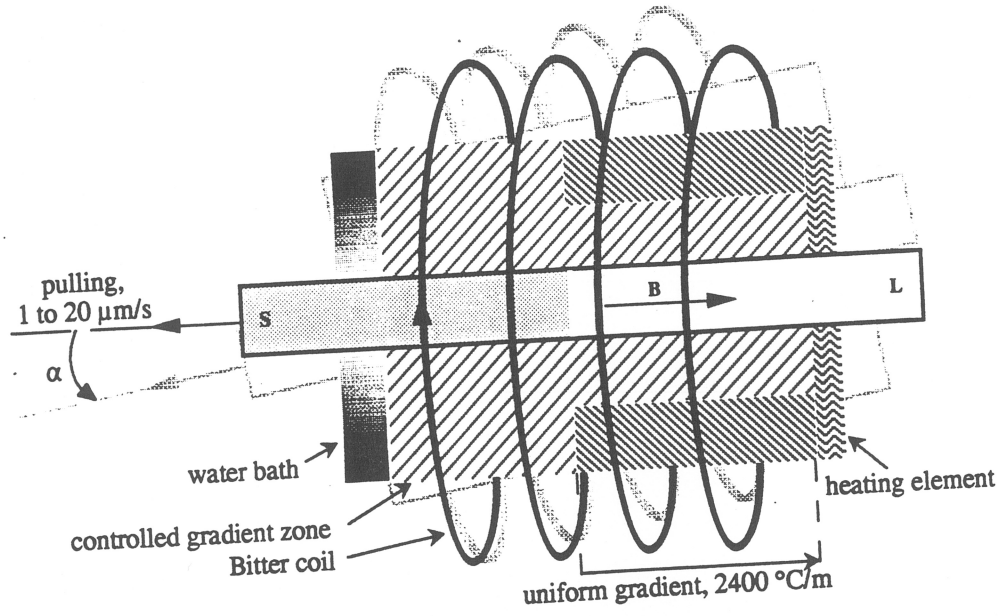

Fig. 1. BRAHMS experimental device.

[1]Commissariat à l'Energie Atomique DTA/CEREM/SES, Centre d'Etudes Nucléaires de Grenoble, 17, av. des Martyrs, 38054 Grenoble Cedex 9, France.
[2]Laboratoire EPM/MADYLAM, ENSHMG, BP 95, 38402 St Martin d'Hères Cedex, France.

Published in Magnitnaya Gidrodinamika, No. 3, pp. 268-275, July-September, 1995.

0024-998X/95/3103-0228$12.50

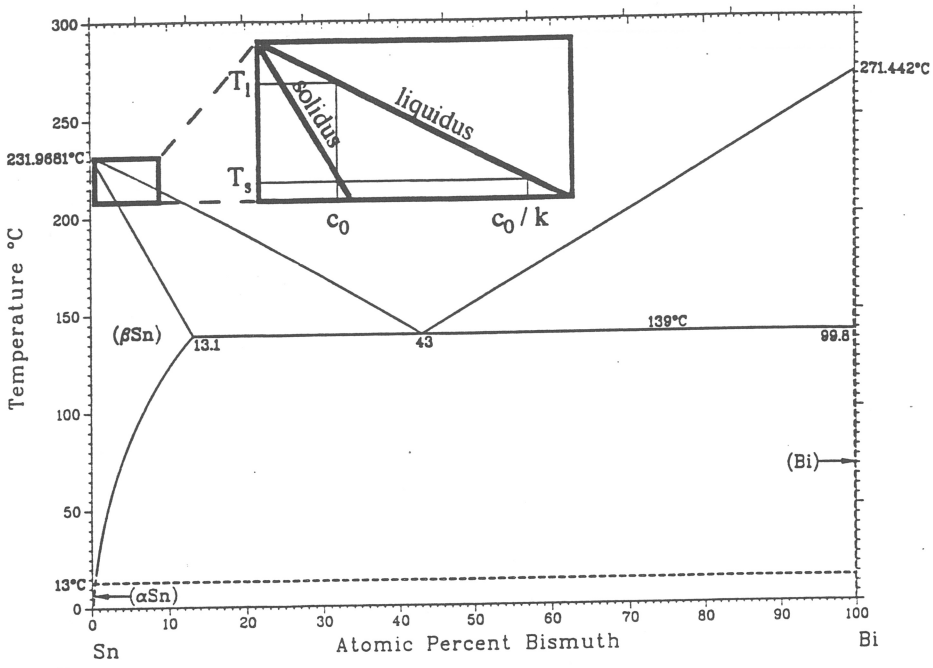

Fig. 2. Phase diagram and solid-liquid equilibrium for a binary system.

The purpose of the BRAHMS (Bridgman Related Apparatus for Hydrodynamic and Magnetic Studies) experiment is to study the effect of a magnetic field in the Bridgman growth of semiconductor or metallic alloys. The characteristic features of BRAHMS are a uniform axial temperature gradient, a uniform axial magnetic field, and a variable orientation with respect to gravity. The experimental device is shown schematically in Fig. 1. The hot and cold zones are separated by a gradient controlled region designed to create a constant axial temperature gradient in the melt, equal to 2400°C/m over a range of 10 cm. Around this furnace is a Bitter coil that creates a uniform steady magnetic field over the same range. The maximum intensity of this field is about 1.3 T. The charge (Ø 6 mm), a tin-bismuth alloy with 0.13 at% Bi – this concentration is imposed by the interface stability criterion – is contained in a quartz crucible ($Ø_{out}$ 10 mm) fixed on the pulling device. The whole device can be tilted from the horizontal position to the vertical at intervals of 15°.

Till now, only the horizontal configuration has been investigated. Since the temperature gradient G is fixed, the Grashoff number $\mathrm{Gr} = g\beta G d^4/\nu^2$ (where g is the intensity of gravity, β the thermal expansion coefficient, d the charge diameter, and ν the kinematic viscosity) is fixed and equal to 46,000. The choice of the alloy determines the Schmidt number, $\mathrm{Sc} = \nu/D = 145$ (D is the solute diffusivity). The experimental parameters are:

– the pulling rate v_i which gives the Pe number; $\mathrm{Pe} = v_i d/D$ ranges from 5 to 100,

– the intensity of the magnetic field B which fixes the Hartmann number; $\mathrm{Ha} = (\sigma/\rho\nu)^{1/2} Bd$ (here σ is the electric conductivity of the liquid and ρ its density) ranges from 0 to 270.

The Gr and Ha numbers are related to the hydrodynamic problem, since Gr scales the buoyancy driving force and Ha the braking electromagnetic force. The Pe and Sc numbers are related to the solutal problem, Pe characterizes the crystal growth rate and the product Gr·Sc measures the convective contribution to mass transfer.

In Sec. 2, we present the mechanism of segregation and introduce the convecto-diffusive parameter D and the effective partition coefficient k_{eff}. The experimental results lead to a value of k_{eff} for given Ha and Pe numbers (Sec. 3). Then we determine the velocity field in the melt which depends on the order of magnitude of the Ha number (Sec. 4). This velocity field can be used as an input in the mass conservation equations and thus allows us to carry out a numerical analysis (Sec. 5). A third approach of the segregation problem consists of an order of magnitude analysis, where we obtain a scaling law Δ(Ha, Pe, Gr·Sc) in the case of the convection controlled regime (Sec. 6). Finally in Sec. 7, we compare the results of these three complementary approaches.

2. Mechanism of Segregation

A local change in the composition occurs due to the equilibrium condition for a binary system containing two phases (Fig. 2): at the solidifying interface, the concentrations in the liquid and the solid are related by the equilibrium distribution coefficient k, $c_{s*} = k \cdot c_{l*}$ [4]. This compositional difference will always lead to concentration variations in the solidified alloy which are known as segregations. Because solute can be transported by diffusion or (and) by convection, the segregation pattern will be different depending upon the process involved.

In a coordinate frame moving at a rate v_i with respect to the laboratory, the governing equations for mass conservation in the bulk and at the solid-liquid interface are

$$\text{bulk: } \partial c/\partial t + (\mathbf{v}\cdot\nabla)c = D\Delta c + (\mathbf{v}_i\cdot\nabla)c, \tag{1}$$

$$\text{interface: } -D\nabla c\cdot\mathbf{n} = c(1 - k)\mathbf{v}_i\cdot\mathbf{n}, \tag{2}$$

where $\mathbf{v}$ is solution of the Navier-Stokes equations. These equations are often very difficult to solve and it is only in highly idealized cases that an analytical solution of Eqs. (1) and (2) can be found.

The first approaches assume complete mixing in the liquid phase which is *a priori* a rather surprising hypothesis, since it is clear from Eq. (2) that there is always a concentration gradient at the interface. But when the growth velocity is very low, the complete mixing hypothesis is likely to be valid. If f_s stands for the solidified fraction, the concentration in the solid is given by

$$c_s(f_s) = kc_0(1 - f_s)^{k-1}, \tag{3}$$

where c_0 is the initial concentration of the feed. This concentration law is often referred to as Scheil's law. Let us notice that it can not be valid over the entire range of f_s when $k < 1$, since the composition will tend to infinity when f_s reaches unity.

A totally different situation occurs when diffusion alone accounts for all mass transport in the melt. Again this appears as a very restrictive hypothesis since convection is always present in all growth processes. But if the growth velocity is high enough, convective transport can be neglected. Then considering that composition is a function of the axial coordinate x alone, Tiller et al. [5] found the solution:

$$c(x) = c_\infty(1 + (1 - k)/k \exp(-xv_i/D)), \tag{4}$$

where c_∞ is the liquid concentration far away from the interface. The composition varies from its value at the interface c_∞/k to c_∞ over a length scale D/v_i; at a distance of a few D/v_i, the concentration in the liquid is uniform and equal to c_∞. Following Wilson [6], we can define the size of the solute boundary layer δ as

$$\delta = (c(0) - c_\infty)/(-\partial c/\partial n\,(n = 0)). \tag{5}$$

In the reference diffusive case, we get $\delta = \delta_D = D/v_i$. In all real cases, the boundary layer thickness takes an intermediate value between 0 and D/v_i, or equivalently, the so-called convecto-diffusive parameter $\Delta = \delta/\delta_D$ varies from 0 to 1. Let us assume that after an initial transient, a quasi-steady state is reached; it is then possible to define an effective partition coefficient:

$$k_{eff} = kc(0)/c_\infty, \tag{6}$$

where $c(0)$ and c_∞ are respectively the concentration at the interface and in the bulk of the fluid. The effective partition coefficient thus ranges from k (complete mixing) to 1 (diffusive regime) depending of course on the intensity of convection in the melt. A very important result is that segregation will always be governed by Scheil's law (3) provided the equilibrium partition coefficient k is changed to the effective partition coefficient k_{eff}. This coefficient is closely related to Δ by the exact relation

$$k_{eff} = k/(1 - (1 - k)\Delta). \tag{7}$$

It is generally easier to estimate the boundary layer thickness from a scaling analysis (see Sec. 6), whereas experimental measurements allow us to estimate an effective partition ratio.

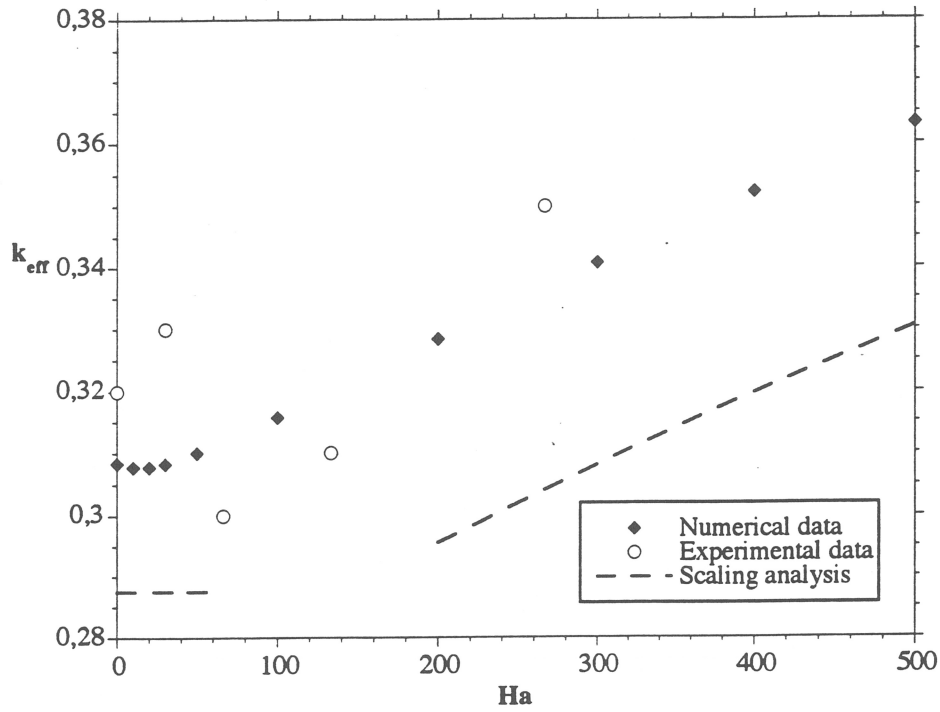

Fig. 3. Segregation for GrSc = 6.7 × 10^6 and Pe = 12.5.

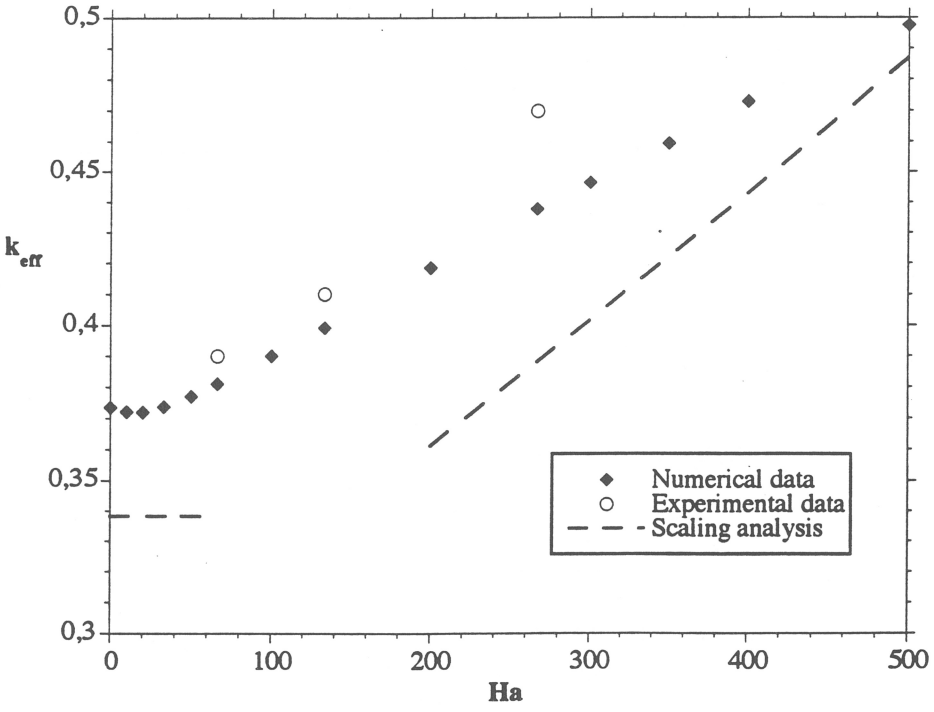

Fig. 4. Segregation for GrSc = 6.7 × 10^6 and Pe = 25.

3. Experimental Results

Our experiments are carried out in the BRAHMS device on Sn−Bi alloys. This means that the Grashoff and Schmidt numbers remain constant; the relevant parameter for segregation studies is their product which takes the value GrSc = 6.7 × 10^6. The equilibrium partition coefficient k is equal to 0.25. We study the influence of the growth velocity and of the imposed axial magnetic field. For growth rates of 2.5 and 5 μm/s, the corresponding Peclet numbers are respectively 12.5 and 25. The importance of the magnetic field is expressed through the Hartmann number which ranges between zero and 270.

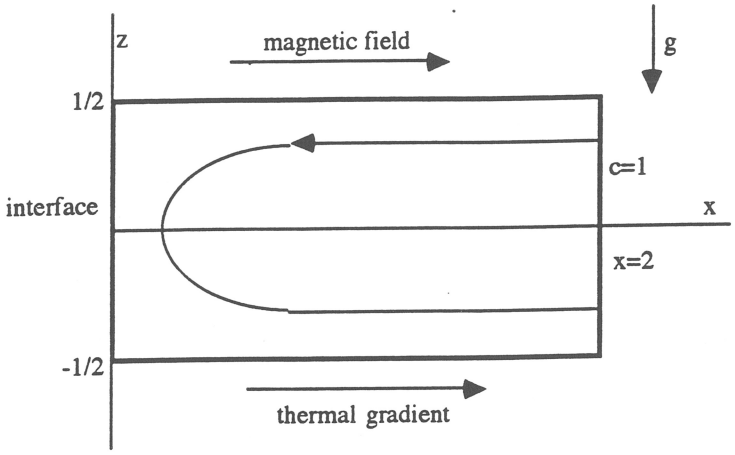

Fig. 5. Geometrical model.

In each growth experiment, controlled solidification is performed on a growth length of 200 mm under stationnary conditions of Pe, GrSc, and Ha numbers, the rest of the alloy sample being not studied. The initial length is about 350 mm. For each solidified sample, 3 mm long pieces are picked along the 200 mm of controlled solidification and their global Bi concentration is measured using an atomic absorption method. Then, using a least square method, we find the best fit of the measured values with Scheil's law.

The measured values are shown on Fig. 3 for Pe = 12.5 and on Fig. 4 for Pe = 25. In the second case of Pe, experiments are carried out for Hartmann numbers equal to 66, 133, and 266 and the effective partition ratio increases slowly. For Pe = 12.5, this ratio seems to grow quickly with Ha (0, 30, and 66), but we are not greatly confident in both the concentration measurements of the first and third Ha value cases since there was not a good correlation with the nearest Scheil's law (as opposed to the other experiments). Further measurements using another method, like ICP (Induced Coupled Plasma), should allow one to get more accurate experimental values.

4. Velocity Field under Magnetic Field

Now, for theoretical as well as numerical modeling of segregation, the knowledge of the velocity field is needed. We only consider the case of a dilute alloy such that convection is purely thermally driven: indeed, the concentration level in our experiments allows us to neglect the buoyancy effects due to the solute gradients. Furthermore, we assume a good thermal conduction and hence a uniform axial thermal gradient in the liquid and a planar growth interface. During BRAHMS experiments, let us recall that uniform conditions of thermal gradient and magnetic field exist along a 10 cm long zone from the solidification front (which is very long compared to the 6 mm diameter).

We model the geometry for the fluid flow as a semi-infinite cylinder bounded with a planar interface. This geometry may also be idealized by considering the vertical mid-plane of the cylinder [7], otherwise stated by assuming the flow between two horizontal plates. This greatly simplifies the modeling since it is now two-dimensional (see Fig. 5).

Even in this simplified configuration, there is no available analytical solution for the steady flow with an axial magnetic field. We have found a Fourier series expansion solution for the velocity. The coefficients could not be obtained in a formal way – they were calculated by an iterative numerical method. This flow presents the following features:

– a Hartmann layer of thickness d/Ha exists along the growth interface, where an important velocity gradient can be observed;

– at a fixed position, say $x = d$ and $z = 0$, the vertical velocity decreases as 1/Ha;

– the length of the recirculating zone increases from one diameter without magnetic field to a length of order $d \cdot$Ha at high Hartmann number.

For the purpose of analytical study of segregation, we observed on the Fourier series expansion that the flow near the interface had the following approximate form:

$$v_z = (\mathrm{Gr} \cdot x/\mathrm{Ha}^2 - \mathrm{Gr}/18\mathrm{Ha}\,(1 - 8z^2 + 16z^4))(1 - \exp(-\mathrm{Ha} \cdot x)), \tag{8}$$

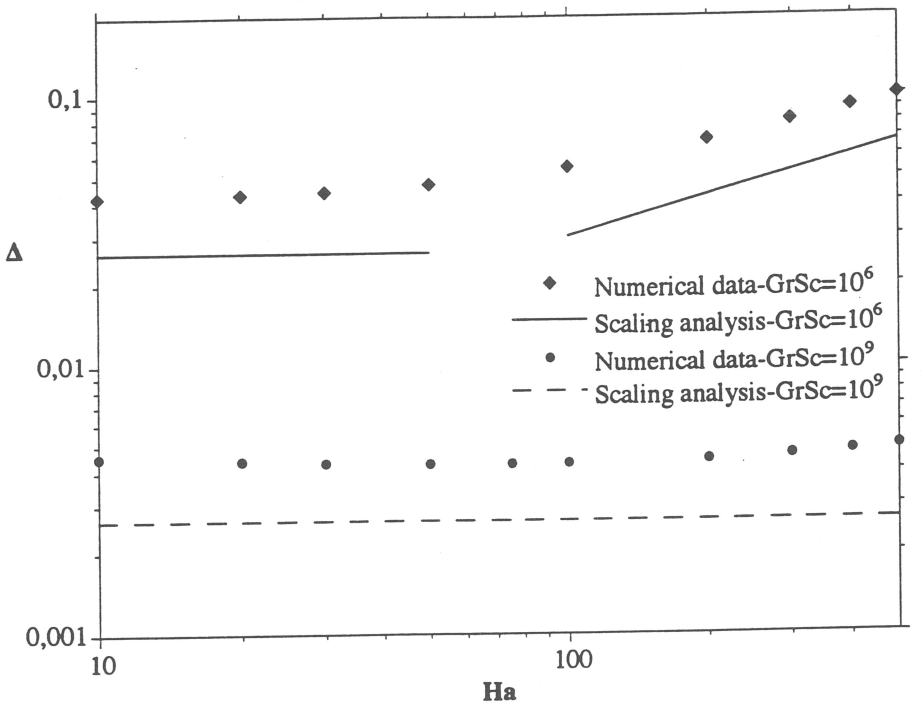

Fig. 6. Segregation for GrSc = 10^6 and 10^9 at Pe = 1.

$$v_x = 8\mathrm{Gr}/9\mathrm{Ha}\,(-xz + 4xz^3) + 8/9\ \mathrm{Gr}/\mathrm{Ha}^2\,(z - 4z^3)(1 - \exp(-\mathrm{Ha}\cdot x)), \tag{9}$$

where the length scale is d and the reference velocity ν/d. These expressions feature the Hartmann layer (factor "1 − exp(—Ha·x)"), the 1/Ha variation of the vertical component of the velocity and the slow variation of v_z with respect to the axial coordinate (factor "Gr·x/Ha^2") hence the Ha length of the recirculating area.

5. Numerical Results of Segregation

Assuming the mean concentration of the melt to change slowly, we consider a quasi-steady model for segregation. At an axial length of two diameters, we imposed a fixed value of unity[1] for the solute concentration. Along the horizontal plates, no solute flux is assumed and at the interface, Eq. (2) applies. Then, Eq. (1) is solved, without the time dependent term, the velocity being given by the Fourier series expansion for a semi infinite cavity derived in Sec. 4. As a result, we get the mean concentration at the interface, which multiplied by the equilibrium partition ratio, leads to the numerical effective partition ratio.

We first solved numerically the segregation problem related to the experimental conditions (see Figs. 3 and 4). Then, we considered two other cases at a unity Peclet number: Gr·Sc = 10^6 and 10^9, for Hartmann numbers from 0 to 500 (see Fig. 6). These numerical results were obtained using the FIDAP software that is based on the finite elements method. We chose a 47 × 49 nodes mesh and rectangular 9 nodes elements. The variable mesh was quite dense near the interface such that the Hartmann layer (at Ha = 500) could extend over several elements.

6. Scaling Analysis

Besides numerical analysis, we have looked for an approximate solution for the axial segregation using a scaling analysis of the segregation Eq. (1). This method has already been successfully applied to growth configurations without a magnetic field by Garandet et al. [8]. Its application requires the knowledge of an approximate solution for the velocity field

[1]It may be any value since our model is linear with respect to the concentration.

near the interface. The purpose of this method is to determine δ, the characteristic solutal layer thickness defined in Sec. 2. In this respect, it is assumed that at the distance δ from the solidification front, the derivative terms along x can be replaced by a division by δ and that the concentration does not greatly vary along z. Then the mean value of Eq. (1) is considered along the upper half cavity at $x = \delta$. This leads to the following equation for the solute layer thickness:

$$Pe - 2Sc \int_0^{1/2} v_x(\delta, z)\, dz = 1/\delta. \tag{10}$$

Solving (10) leads to a value for δ when v_x is replaced using expression (9). In the following, we restrict ourselves to the convective case, for which the first term of (10) can be neglected: this is the case of a small solute layer thickness compared to the diffusive case. Then two cases may be distinguished. The solute layer may be contained in the Hartmann layer, or on the contrary, the Hartmann layer thickness may be small compared to that of the solute. In the first case, the exponential velocity profile is linearized, leading to the following expression for Eq. (10), in terms of Δ:

$$\Delta \approx 2.62\mathrm{Pe}(\mathrm{GrSc})^{-1/3}. \tag{11}$$

In the second case, the Hartmann layer is not taken into account and Eq. (10) writes

$$\Delta \approx 3\mathrm{Pe}(\mathrm{GrSc})^{-1/2}\mathrm{Ha}^{1/2}, \tag{12}$$

These results can be used to determine *a posteriori* the validity field of each *regime*. It is easily found that for Hartmann numbers less than $0.5(\mathrm{Gr}\cdot\mathrm{Sc})^{1/3}$ Eq. (11) holds and otherwise, Eq. (12) is valid. The scaling analysis results on Figs. 3, 4 and 6 are shown to compare well with numerical calculations, and in particular, the two distinct *regimes* are present on Fig. 6 in the case of $\mathrm{Gr}\cdot\mathrm{Sc} = 10^6$. The threshold Ha value separating them is about 50, according to the $0.5(\mathrm{Gr}\cdot\mathrm{Sc})^{1/3}$ estimate. On the contrary, for the case of $\mathrm{Gr}\cdot\mathrm{Sc} = 10^9$, only the first *regime* is observed, even for Ha values up to 500.

7. Conclusion

Further experimental results are certainly needed to ensure the validity of both numerical and scaling analysis results, which are in good agreement together. It is of great interest to notice the existence of a minimum Ha value depending on $\mathrm{Gr}\cdot\mathrm{Sc}$ under which the axial magnetic field has no inflence on the axial segregation: numerical results show that this segregation may even be slightly enhanced under a magnetic field. Then above this value, in the convective limit, the convecto-diffusive parameter Δ grows at the rate $\mathrm{Ha}^{1/2}$, which may be compared to the 1/Ha reduction of the velocity field. It can be considered that an axial magnetic field is not an efficient tool to reduce axial segregation, especially at high $\mathrm{Gr}\cdot\mathrm{Sc}$ values.

For high growth rates (10 to 20 μm/s) the morphological stability threshold is exceeded and the Bi concentration must be reduced to 0.04 at%. Otherwise the Grashoff number can be artificially modified by tilting the experimental device, angles of 60 and 75° dividing Gr by 2 each time. These experiments will be carried out in the near future.

In the vertical position, the problem is quite different since convection close to the solidification front is driven by radial temperature gradients due to interface curvature [9], [10]. The first experiments showed that the radial temperature gradients in the BRAHMS furnace are weak since in all cases the solidification was diffusion controlled. Another experimental configuration that should be studied is the case of a transversal magnetic field: a second furnace of the same type is available and should be adapted to the transverse electromagnet of the MASCOT experiment at the Madylam laboratory in Grenoble.

REFERENCES

1. W. E. Langlois, "Buoyancy driven flows in crystal growth melts," *Ann. Rev. Fluid Mech.*, **17**, 191-215 (1985).

2. J. A. Burton, R. C. Prim, and W. P. Schlichter, "The distribution of solute in crystals grown from the melt," *J. Chem. Phys.*, **21**, 1987-1996 (1953).
3. C. Vives and C. Perry, "Effects of magnetically damped convection during the controlled solidification of metals and alloys," *Int. J. Heat Mass Transfer*, **30**, 479-496 (1987).
4. M. C. Flemmings, Solidification Processing, *McGraw Hill*, New York (1974).
5. W. A. Tiller, K. A. Jackson, J. W. Rutter, and B. Chalmers, "The redistribution of solute atoms during the solidification of metals," *Acta Met.*, **1**, 428-437 (1953).
6. L. O. Wilson, "On interpreting a quantity in the Burton, Prim and Schlichter equation as a diffusion boundary layer thickness," *J. Cryst. Growth*, **44**, 247-250 (1978).
7. P. Bontoux, B. Roux, G. H. Schiroky, B. L. Markham, and F. Rosenberg, "Convection in the vertical midplane of a horizontal cylinder. Comparison of two-dimensionnal approximations with three-dimensionnal results," *Int. J. Heat Mass Transfer*, **29**, No. 2, 227-240 (1986).
8. J. P. Garandet, T. Duffar, and J. J. Favier, "On the scaling analysis of the solute boundary layer in idealized growth configurations," *J. Cryst. Growth*, **106**, 437-444 (1990).
9. M. Adornato and R. A. Brown, "Convection and segregation in directional solidification of dilute and non-dilute binary alloys: effects of ampoule and furnace," *J. Cryst. Growth*, **80**, 155-190 (1987).
10. S. Motakef, "Magnetic field elimination of convective interference with segregation during vertical Bridgman growth of doped semi-conductors," *J. Cryst. Growth*, **104**, 833-850 (1990).